An AFM study on ferroelastic domains in lead phosphate, $Pb_3(PO_4)_2$

1997 J. Phys.: Condens. Matter 9 8397

(http://iopscience.iop.org/0953-8984/9/40/007)

J. Phys.: Condens. Matter **9** (1997) 8397–8405. Printed in the UK PII: S0953-8984(97)84096-9

An AFM study on ferroelastic domains in lead phosphate, $Pb_3(PO_4)_2$

Dirk Bosbach†, Andrew Putnis†, Ulrich Bismayer‡ and Bernd Güttler§

† Institut für Mineralogie, Universität Münster, Corrensstrasse 24, 48149 Münster, Germany
‡ Mineralogisch Petrographiches Institut, Universität of Hamburg, Grindelallee 48, 20146 Hamburg, Germany
§ PTB, Burchallee 100, 38116 Braunschweig, Germany

Received 7 May 1996

Abstract. The topography of the intersection of ferroelastic W domain walls with (100) surfaces of lead phosphate, $Pb_3(PO_4)_2$, has been imaged with tapping mode atomic force microscopy (TMAFM). Spontaneous deformation of the ferrophase leads to a cleavage plane which forms a zig-zag profile along W domain walls. The predicted angle of 178.55° between two adjacent domains on a (100) surface is confirmed by TMAFM observations. Surface deformation has no influence on this angle due to the dominance of the long-range spontaneous strain. Furthermore, W domains end as needle-like structures and TMAFM observations show that there is no detectable change in the local surface deformation in the vicinity of these needle tips.

1. Introduction

Ferroelasticity appears below a critical temperature T_C and leads to the formation of domains. These domains are macroscopic deformation states described by the supergroup–subgroup relation of the corresponding ferroic system transforming from a paraphase to a ferrophase. Domains in the ferrophase represent energetically equivalent orientation states given by spontaneous strain tensors [1, 2]. In soft ferroelastics mechanically different domains can be reoriented by the application of external stress.

The integration over all ferroelastic domains leads to a pseudosymmetric average symmetry which corresponds to the paraphase symmetry. Ferroelastic domains are separated by walls with finite width [3]. Sapriel [4] showed that all permissible walls are described by symmetry operations of the prototype phase which do not belong to the ferrophase. The walls were described as plane walls with an orientation predictable from the ferroelastic strain. The reorientation of the critical quantities, i.e. the strain between neighbouring domains, has been considered on an atomic level as dislocations such that the lattices on either side of the wall correspond to each other by a simple rotation referred to a coordinate system linked to the wall [5]. This approach allowed the description of the intersection of perpendicular running walls of different type classified as W and W′. Experimental observations of the domain structure morphology showed, however, that theoretically predicted angle characteristics can in real crystals strongly deviate from the ideal angles [6]. Modern HRTM studies on such domain formations lead to theoretical descriptions which require gradient terms and complex elasticity theory to describe the picture on a local scale [7].

0953-8984/97/408397+09$19.50

One of the best studied ferroelastic model systems with precisely determined strain tensor components and domain structure is lead phosphate, $Pb_3(PO_4)_2$ [3, 4, 8–12]. The global symmetry reduction of improper ferroelastic lead phosphate is $R\bar{3}m$–$C2/c$. The ferroelastic transition has been described using a three state Potts model [13]. The structure of the high-temperature phase consists of interconnected chains PO_4–Pb(2)–Pb(1)–Pb(2)–PO_4 parallel to the threefold inversion axis. The monoclinic ferrophase is characterized by displaced lead atoms perpendicular to the threefold axis, parallel to the binary axis of the $C2/c$ phase and weakly deformed PO_4 tetrahedra [14]. The material belongs to the ferroelastic species with $\bar{3}mF2/m$ domain pattern described by W and W′ walls corresponding to pseudomirror planes and pseudobinary axis respectively. Because of the ferroelastic deformation the (100) cleavage plane of lead phosphate crystals appears to be bent at the trace of W walls. The aim of the present work is to visualize the resulting three-dimensional pattern in ferroelastic lead phosphate for the first time using atomic force microscopy. Geometrical features and theoretically predicted deformation states are discussed.

The W walls represent pseudomirror planes, namely $(11\bar{3})$ and $(1\bar{1}\bar{3})$ in the monoclinic phase. The W′ walls contain the pseudobinary axis [011] or $[01\bar{1}]$ and separate ferroelastic orientation states by a 120° rotation around the $[\bar{1}11]$ axis or by 60° in corresponding intersections (figure 1). W and W′ walls show perpendicular intersections [15]. The rotation angles of neighbouring domain lattices differ by an angle

$$\omega = \sqrt{3(e_{11}^2 + e_{13}^2)}$$

from the ideal angles predicted by the symmetry reduction [5, 6, 9].

Because of small non-stoichiometries in lead phosphate crystals zig-zag shaped W wall configurations were observed [15, 16]. The zig-zag shaped W domains show a typical wall–wall distance of ∼0.020 mm in $Pb_3(PO_4)_2$ and decreasing distance with increasing impurity concentration. The rotation angle ω leads to a curvature of the needle tips which decreases with increasing temperature and vanishes at the ferroelastic transition point together with the domains. A system of zig-zag domains shows a typical strain profile described by a tanh form similar to that of a single W′ domain running perpendicular to it [15].

The orientation of the walls in the bulk is described by simple geometrical relations of the lattices and symmetry elements below and above the ferroelastic transition point. The angle between the monoclinic binary axis [010] and the trace of the W walls along [031] on the cleavage plane (100) is

$$\tan\varphi = c_{mon}/(3b_{mon}).$$

The angle φ is 30° in the paraphase of lead phosphate and 28.92° at room temperature [10]. Because of the spontaneous deformation of the ferrophase the angle between the pseudomirror plane W and the cleavage plane (100) is less than 90°. The exact value for lead phosphate is 89.275°. This leads to a cleavage plane which forms in fact a slight zig-zag profile along the W wall (figure 2). Instead of 180° an angle of 178.55° joins the (100) plane on either side of the wall. The profile can vary in case of inhomogeneous strain distribution and with the density of the walls. However, it is not clear whether the 178.55° degree angle, which has been predicted from bulk properties, does actually appear on $Pb_3(PO_4)_2$ surfaces or whether it is different due to the local surface deformation.

First AFM images of ferroelectric and ferroelastic domains have been published previously [17–19]. In this paper we describe the inclination angle of the surface and the changes of the angle on approaching a needle tip, studied with tapping mode atomic force microscopy.

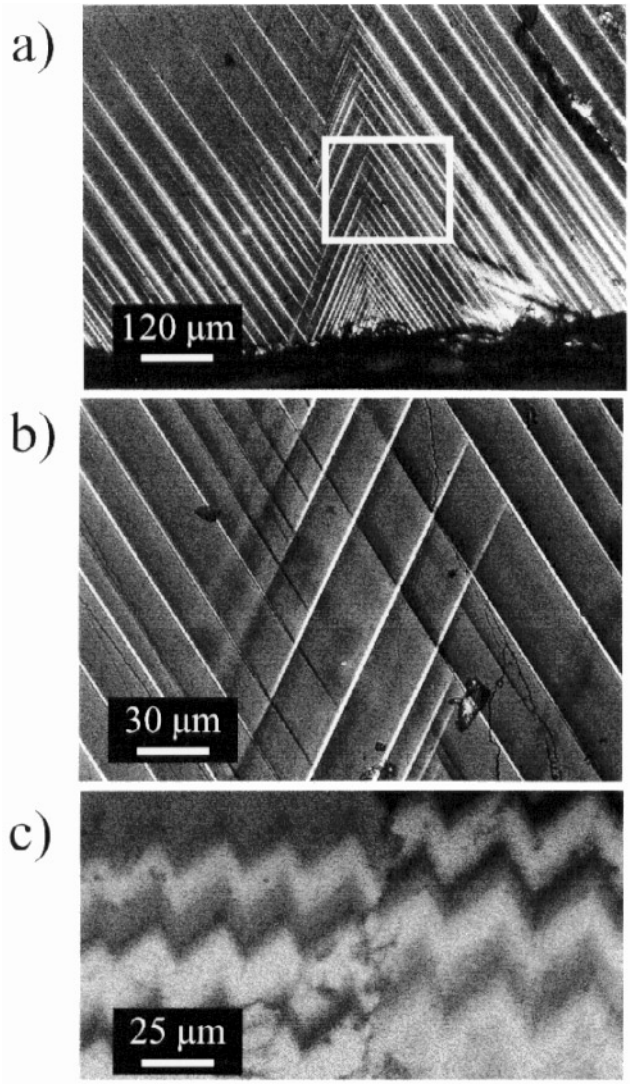

Figure 1. (a) Ferroelastic W domains in $Pb_3(PO_4)_2$ under an optical microscope with crossed polarizers. (b) Closeup view of the marked area in (a). (c) Optical Mireau interference pattern on a (100) surface of $Pb_3(PO_4)_2$.

2. Experimental details

Atomic force microscopy (AFM) is a technique which provides quantitative topographic data of solid surfaces. A sharp tip, which is attached to a cantilever-like spring, tracks the sample surface with sub-nanometre resolution. Therefore, molecular topographic features on a solid surface can be imaged on a routine basis. Tapping mode atomic force microscopy (TMAFM) is a new AC mode of operation, where the tip oscillates vertically near its resonance frequency, with the tip slightly tapping the sample surface. Consequently, the amplitude of the oscillating tip is reduced compared to the amplitude of free oscillation without tapping the sample surface [20]. In TMAFM this change of amplitude is used to

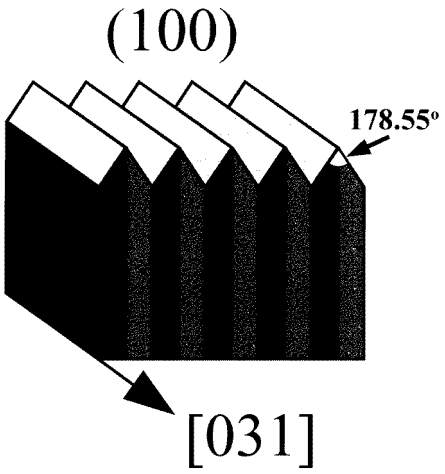

Figure 2. Ferroelastic W domains in $Pb_3(PO_4)_2$. The domains are oriented parallel to [031]. Due to the spontaneous deformation of the ferrophase the angle between W and the cleavage plane (100) if less than 90°. A (100) cleavage surface forms a zig-zag profile with a typical angle of 178.55°.

track the sample topography. The tip–sample interaction is significantly reduced compared to conventional contact mode AFM and potential tip artefacts due to high loading forces (e.g. friction, sample destruction) do not occur.

We have used a Digital Instruments Dimension 3000 AFM with Si single-crystal high-aspect-ratio tips. Cleaved $Pb_3(PO_4)_2$ samples were mounted on a glass mount, thus enabling us to select suitable sample areas optically (with crossed polarizers) before imaging that same area with TMAFM. The amplitude of the oscillating cantilever was reduced only slightly during imaging (soft tapping). Piezo creep of the AFM scanner potentially results in incorrect topographic data of the sample surface. Since quantitative information about the sample surface is crucial in order to confirm theoretical predictions about the surface deformation, we have applied slow scan rates of $\leqslant 0.2\ s^{-1}$ at a scan size of 25 μm resulting in a scan speed of about 5 $\mu m\ s^{-1}$.

3. Results and discussion

Ferroelastic domains in $Pb_3(PO_4)_2$ can be observed optically using crossed polarizers, due to their reoriented optical indicatrices and slight distortion in the bulk (figure 1(a), (b)). Additionally, due to the spontaneous deformation of the ferrophase the angle between W and the cleavage plane (100) is $\neq 90°$. The (100) cleavage surface forms a zig-zag profile with a typical angle of 178.55° (figures 1(c), 2). The optical Mirau-interference pattern using a commercial interferometer and an optical microscope confirms the narrow zig-zag pattern of the (100) surface (figure 1(c)). The theoretically derived value is very well confirmed in the limits of error (±0.2°) by TMAFM observations of freshly cleaved $Pb_3(PO_4)_2$ surface (figures 3, 4). The ferroelastic domains were mechanically induced before cleaving the sample. Molecular steps clearly run across the domain boundary. Detailed topographic analysis in the vicinity of W walls show that they appear as rounded surface features in TMAFM images with a radius of curvature of about 50 nm rather than as sharp edges. However, in TMAFM a tip with a finite end radius of curvature scans the sample

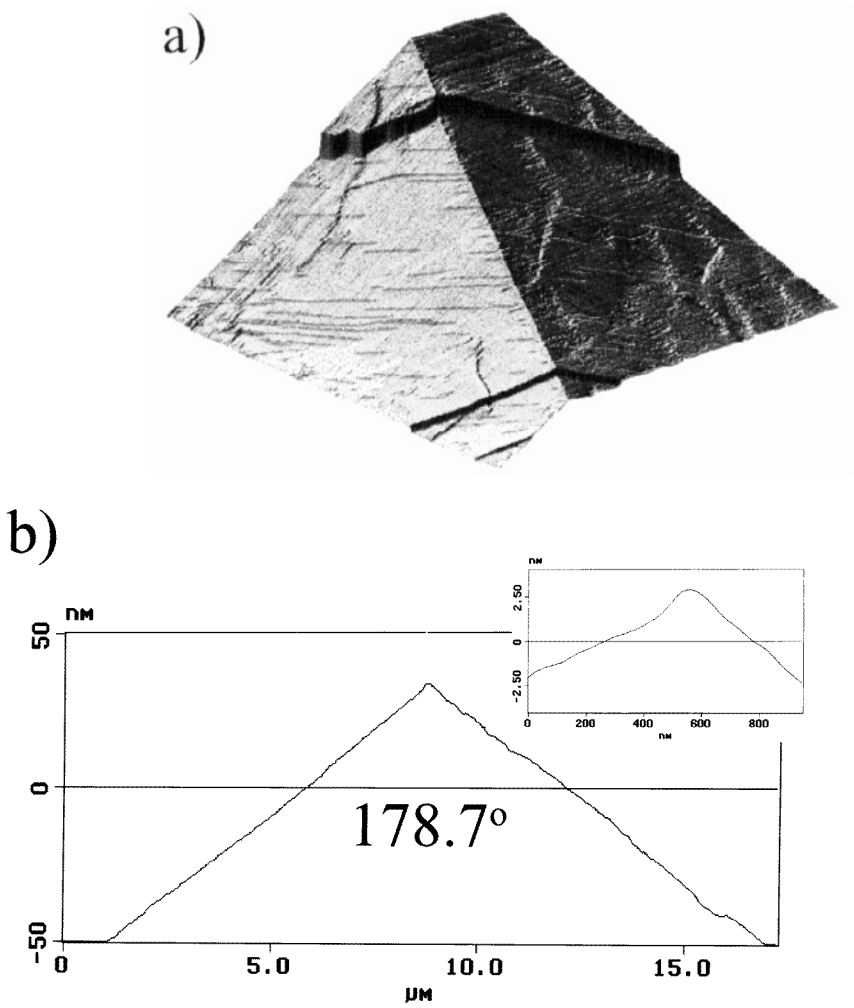

Figure 3. (a) TMAFM image of two ferroelastic domains in $Pb_3(PO_4)_2$ forming a wedgelike feature on the (100) surface (scan size: 15×15 μm^2). Molecular cleavage steps are clearly visible as well as macro-steps. (b) The angle between these domains is about 178.7°, which agrees quite well with the theoretically predicted value of 178.55°. On a smaller scale the W domain wall appears as a curved surface feature (see inset).

surface and it is a common phenomenon in scanning probe microscopy that sample surface features which are sharper than the AFM tip are not imaged perfectly [21]. The AFM tip is actually imaged by the sample surface! Therefore, we have used Si high-aspect-ratio tips with a radius of curvature of approximately 10–20 nm which is smaller than the observed radius of curvature of the $Pb_3(PO_4)_2$ surface in the vicinity of W domain walls and hence an imaging artefact can be excluded. However, the $Pb_3(PO_4)_2$ surface might have been altered chemically and the observed rounded surface features may not represent the original unaltered surface. It is well known that crystal surfaces can be quite reactive when exposed to ambient conditions [22]. However, recent theoretical concepts [23] consider the possibilities of transient pattern dynamics and nonlinear, nonequilibrium

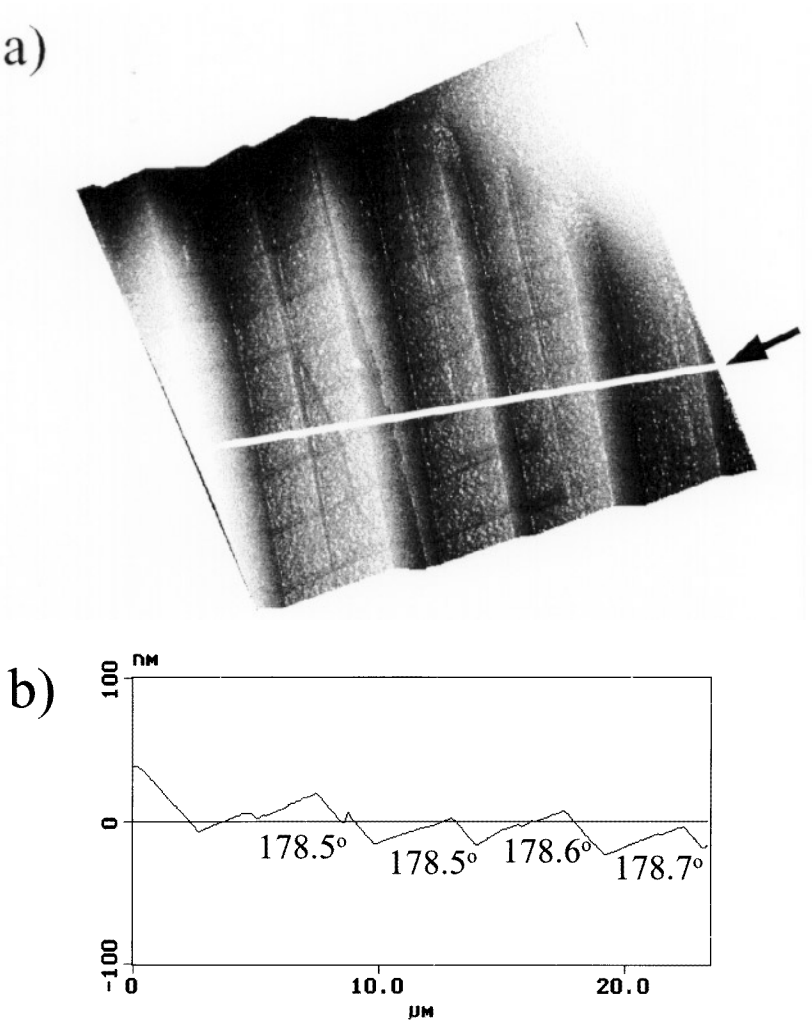

Figure 4. (a) Ferroelastic W domains on a (100) surface of $Pb_3(PO_4)_2$ (scan size: $22 \times 22\ \mu m^2$). (b) Cross-section along the indicated line in (a). The angle between these domains is in the range of 178.5° even though the domain size is smaller compared to the domains shown in figure 3.

phenomena of domain formations leading to wall bending. Houchmandzadeh *et al* [24] correlated interfaces and ripple states of domain walls with metastable modulated textures in ferroelastic crystals close to the crystal surface. Our observations may therefore show the correct lattice relaxation with modulations close to the wall.

In addition to simple parallel W domain configurations we have imaged the surface of the complex arrangements of W domains, which have been observed optically (figure 1(b)) and with TMAFM (figure 5(a)). Again, molecular as well as macro steps are clearly visible. In figure 5(b) the TMAFM amplitude data are given in addition to the height data (figure 5(a)). TMAFM amplitude data basically represent the error signal of the feedback loop system which keeps the amplitude of the oscillating tip constant while scanning over the sample surface, thus tracking the surface topography. Therefore, geometrically uniform oriented

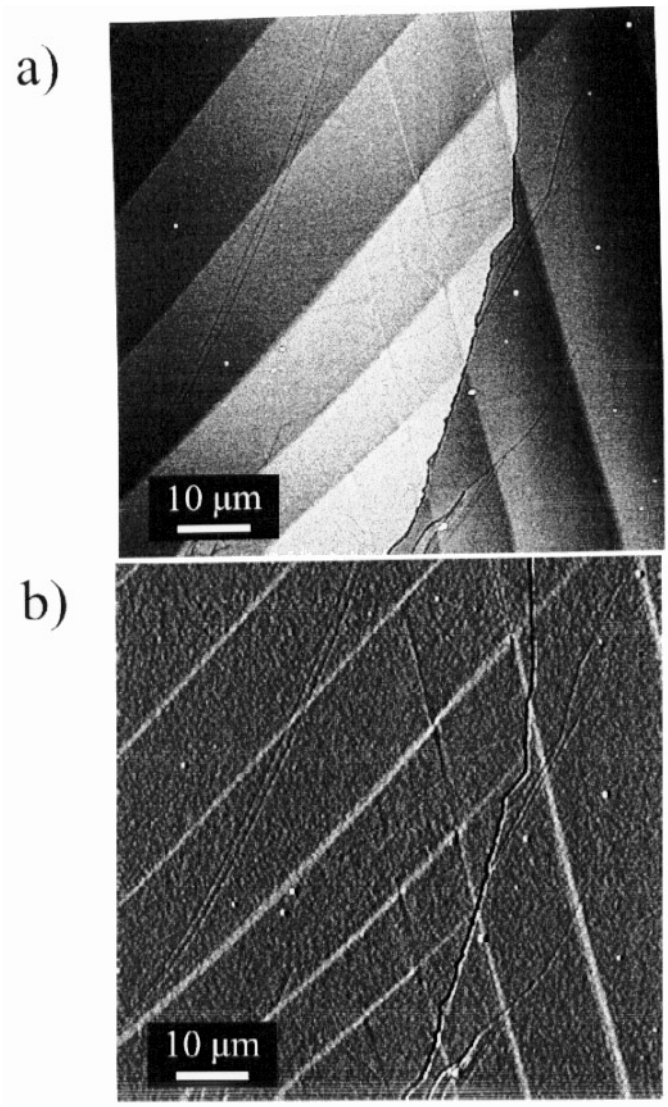

Figure 5. (a) TMAFM height data of ferroelastic W domains on a (100) surface of $Pb_3(PO_4)_2$ (scan size: 80×90 μm^2). (b) Amplitude data of the same surface area. Since amplitude data represent the error signal of the feedback loop, grey scales indicate surface tilt.

surface areas, e.g. W domains with constant tilt angle, result in a constant error signal and are displayed with the same colour in the amplitude data representation (figure 5(b)). Thus bright areas represent thin domains with adjacent wider domains (dark) having constant surface tilt.

The W domains end as needle-like structures which can be clearly seen optically and in TMAFM images (figures 1, 6). Such wall profiles in materials with pinning centres have been treated theoretically by Salje and Ishibashi [25]. Based on the Landau–Ginzburg and elasticity theory the authors calculated wall trajectories and their tip curvature for needle domains. Our experiments verify for the first time the profile of an anisotropy-dominated needle with a parabolic trajectory (for details see [25]). TMAFM amplitude data show that

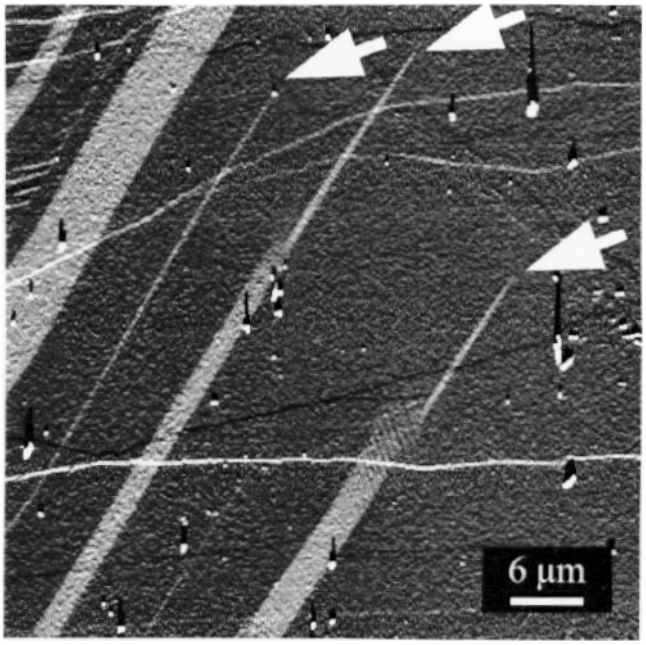

Figure 6. TMAFM amplitude data of ferroelastic W domains on a (100) surface of $Pb_3(PO_4)_2$ (scan size: 60×60 μm^2). The W domains end as needle-like structures—indicated by arrows. There is no detectable change in the local surface deformation in the vicinity of a needle tip.

there is no detectable change in the local surface deformation in the vicinity of a needle end. Furthermore, our observations confirm no change in the tilt angle of adjacent W domains even for changing wall–wall distances. However, since the limits of error observations of the tilt angle is about 0.2°, a smaller change cannot be excluded (figure 6).

In conclusion, TMAFM is a powerful method for studying the surface deformation of ferroelastic materials. The observed inclination angle on the (100) surface of $Pb_3(PO_4)_3$ confirms well the theoretically predicted value of 178.55°. Obviously, the surface deformation has no detectable influence on that angle because of the dominance of the long-ranging spontaneous strain. Furthermore, on the scale of our observations, we have even not detected local changes of that angle in the vicinity of W domain needle ends which agrees well with the predictions by Salje and Ishibashi [25]. Combined TMAFM height data and amplitude data are therefore ideal for representing the regular zig-zag profile of materials with large 'strain' tensor components, like $Pb_3(PO_4)_2$ with $\varepsilon_{11} \approx 2\%$.

References

[1] Aizu K 1970 Determination of state parameters and formulation of spontaneous strain for ferroelastics *J. Phys. Soc. Japan* **28** 706
[2] Kleemann M and Schlenker M 1972 Use of elasticity theory in magnetoelasticity *J. Appl. Phys.* **43** 3184
[3] Wruck B, Salje E K H, Zhang M, Abraham T and Bismayer U 1994 On the thickness of ferroelastic twin walls in lead phosphate $Pb_3(PO_4)_2$ a x-ray diffraction study *Phase Transitions* **48** 135
[4] Sapriel J 1975 Domain wall orientations in ferroelastics *Phys. Rev.* B **12** 5128
[5] Torres J, Roucau C and Ayroles R 1982 Investigation of the interactions between ferroelastic domain walls and of the structural transition in lead phosphate observed by electron microscopy. I: experimental results *Phys. Status Solidi* **70** 695

[6] Dudnik E F and Shualov L A 1989 Domain structure and phase boundaries in ferroelastics *Ferroelastics* **98** 207
[7] Salje E K H 1993 *Phase Transitions in Ferroelastic and Co-elastic Crystals* (Cambridge: Cambridge University Press)
[8] Guimaraes D M C 1979 Ferroelastic transformations in lead orthophosphate and its structure as a function of temperature *Acta Crystallogr.* A **35** 108
[9] Wood I, Wadhavan V K and Glazer A M 1980 Temperature dependence of spontaneous birefringence in ferroelastic lead orthophosphate *J. Phys. C: Solid State Phys.* **13** 5155
[10] Bismayer U and Salje E 1981 Ferroelastic phases in $Pb_3(PO_4)_2$–$Pb_3AsO_4)_2$ *Acta Crystallogr.* A **37** 145
[11] Bismayer U, Salje E and Joffrin C 1982 Reinvestigation of the stepwise character of the ferroelastic phase transition in lead phosphate–arsenate *J. Physique* **43** 119
[12] Salje E, Graeme-Barber A, Carpenter M A and Bismayer U 1993 Lattice parameters, spontaneous strain and phase transition in $Pb_3(PO_4)_2$ *Acta. Crystallogr.* B **49** 387
[13] Salje E and Devarajan V 1981 Potts model and phase transition in lead phosphate $Pb_3(PO_4)_2$ *J. Phys. C: Solid State Phys.* **14** L1029
[14] Keppler U 1970 Struktur der Tieftemperaturform des Bleiphosphates *Z. Kristallogr.* **132** 228
[15] Bismayer U, Hensler J, Salje E and Güttler B 1994 Renormalization phenomena in Ba-diluted ferroelastic lead phosphate, $(Pb_{1-x}Ba_x)_3(PO_4)_2$ *Phase Transitions* **48** 207
[16] Bleser T, Berge B, Bismayer U and Salje E K H 1994 The possibility that the optical second-harmonic generation in lead phosphate, $Pb_3(PO_4)_2$, is related to structural imperfections *J. Phys.: Condens. Matter* **6** 2093
[17] Takashige M, Hamazaki S I, Fukurai N, Shimizu F and Kojima S 1995 Atomic force microscope observations of ferroelectrics: barium titanate and Rochelle salt *Japan. J. Appl. Phys.* **35** 5181
[18] Tsunekawa S, Hara K, Hishitani R, Kasuya A and Fukuda T 1995 Observation of ferroelastic domains in $LaNbO_4$ by atomic force microscope *Mater. Trans. JIM* **316** 1188
[19] Hamazaki Si, Shimizu F, Kojima S and Takashige M 1996 Ferroelectric domains studied by atomic force microscopy *J. Korean Phys. Soc.* **29** S503
[20] Magonov S N and Whangbo M 1996 *Surface Analysis with STM and AFM* (New York: VCH)
[21] Keller D J and Franke F S 1993 Envelope reconstruction of probe microscope images *Surf. Sci.* **294** 409
[22] Stipp S L S, Eggleston C M and Nielsen B S 1994 Calcite surface structure observed at microtopographic and molecular scales with atomic force microscopy (AFM) *Geochim. Cosmochim.* **58** 3023
[23] San Miguel M, Amengual A and Hernan dez-Garcia E 1994 Transient pattern dynamics and domain growth *Phase Transitions* **48** 65
[24] Houchmandzadeh B, Lajzerowicz J and Salje E K H 1991 Order parameter coupling and chirality of domain walls *J. Phys.: Condens. Matter* **3** 5163
[25] Salje E K H and Ishibashi Y 1996 Mesoscopic structures in ferroelastic crystals: needle twins and right angle domains *J. Phys.: Condens. Matter* **8** 8477